UNITED NATIONS

EP

UNEP/MED WG.550/Inf.13

United Nations Environment Programme Mediterranean Action Plan

Distr.: General
17 February 2023

English only

Integrated Meeting of the Ecosystem Approach Correspondence Groups (CORMONs)

Athens, Greece, 27-28 June 2023

Agenda Item 1.C.i-iii: Review of the 2023 Med QSR: the proposal of the IMAP Pollution Cluster Chapters

The Marine Environment Assessment in the Areas with Insufficient Data: The Assessment Results of IMAP Common Indicators 14 in the Central Mediterranean Sea Sub-region by Applying the Simplified G/M Assessment Methodology

UNEP/MAP
Athens, 2023

Table of Contents

List of Abbreviations / Acronyms

AEL	Aegean-Levantine Sea
AZ	Assesment Zones
CEN	Ionian Sea and Central Mediterranean Sea Sub-region
Chl *a*	Chlorophyll *a*
CI	Common Indicator
COP	Conference of the Parties
CORMON	Correspondence Group on Monitoring
CPs	Contracting Parties
DIN	Dissolved Inorganic Nitrogen
EIONET	European Environment Information and Observation Network
EO	Ecological Objective
ESRI	Environmental Systems Research Institute
EU	European Union
GES	Good Environmental Status
nonGES	not Good Environmental Status
IMAP	Integrated Monitoring and Assessment Programme of the Mediterranean Sea and Coast and Related Assessment Criteria
MAP	Mediterranean Action Plan
MED POL	Programme for the Assessment and Control of Marine Pollution in the Mediterranean Sea
MED QSR	Mediterranean Quality Status Report
MSFD	Marine Strategy Framework Directive
MSs	Member States
NEAT	Nested Environmental Assessment Tool
SAU	Spatial Assessment Unit
TP	Total Phosphorous
WMS	Western Mediterranean Sea

1. Introduction

1. To implement the recommendations of the Meeting of CorMon on Pollution Monitoring (Teleconference, 26-27 April 2021) and the Meeting of the MEDPOL Focal Points (Resumed Session, 9 July 2021), the methodologies proposed for assessment of eutrophication were tested in the Adriatic Sea Sub-region. Along with the application of the NEAT assessment methodology in the Adriatic Sea Sub-region, and further to data availability, the application of the Ecological quality ratio (EQR); the Simplified EQR methodology, and the Simplified methodology based on G/M comparison was also explored in other three Mediterranean Sub-regions.

2. The application of the EQR methodology was found relevant for assessment of IMAP Common Indicators 13 and 14 where full set assessment criteria for Chl *a*, DIN and TP exist. It is also necessary to perform the typology related assessment. Given the lack of data reported by the CPs, this methodology was impossible to apply for any sub-region/sub-division of the Mediterranean within the preparation of the 2023 MED QSR.

3. The application of the simplified EQR methodology was found relevant where complementary data availability i.e. *in situ* and from remote sensing is found for Chla only and the typology related assessment is not possible to apply. Due to absence of the homogenous quality assured data reported by the CPs even for Chla only, an application of the simplified EQR method was also impossible for any sub-region/sub-division of the Mediterranean within the preparation of the 2023 MED QSR.

4. Given the lack of quality-assured, homogenous data prevented the application of both EQR and simplified EQR assessment methodologies, the assessment of eutrophication within the preparation of the 2023 MED QSR was undertaken in the sub-divisions of the Aegean-Levantine Sea (AEL), the Ionian Sea and Central Mediterranean Sea (CEN) and the Western Mediterranean Sea (WMS) by evaluating only data for Chla available from the remote sensing sources, whereby the typology-related assessment was impossible to apply.

5. The application of this Simplified methodology and based on G/M comparison in the CEN relied on the use of COPERNICUS data for Chl *a* obtained by remote sensing.

2. Data availability and elaboration

6. A detailed data analysis was performed in order to decide on applying the assessment methodologies that can be found optimal for specific sub-region/sub-division in the present circumstances related to the lack of data reporting. Table 1 informs on data availability in CEN by considering data reported by the Contracting Parties by 31st October, the cut-off date for data reporting. Figure 1 shows the locations of sampling stations in the CEN Sub-region.

Table 1. Data availability by country and year for the Ionian Sea and Central Mediterranean Sea (CEN) Sub-region showing data reported by the CPs for the assessment of EO5 (CI13 and CI14) up to 31st Oct 2022.

<table>
<tr><th>Country</th><th>Year</th><th>Amon</th><th>Ntri</th><th>Ntra</th><th>Phos</th><th>Tphs</th><th>Slca</th><th>Cphl</th><th>Temp</th><th>Psal</th><th>Doxy</th></tr>
<tr><td>Greece</td><td>2016-2021</td><td colspan="10">No data provided</td></tr>
<tr><td rowspan="6">Italy</td><td>2016</td><td colspan="10" rowspan="6">By 31st October 2022, Italy reported data relevant to the Central Mediterranean Sea Sub-region, in 4 data files with all together 260 208 data points up to 2018-2019 On 16 Dec 2022 data for 2020 were also provided. Without building of a dedicated quality assured database, it is impossible to analyse the data availability and ensure their use for the assessment. It should be noted that quantum of data reported guarantees a near monthly sampling frequency on 11 profiles with 4 stations.</td></tr>
<tr><td>2017</td></tr>
<tr><td>2018</td></tr>
<tr><td>2019</td></tr>
<tr><td>2020</td></tr>
<tr><td>2021</td></tr>
<tr><td>Libya</td><td>2016-2021</td><td colspan="10">No data provided</td></tr>
<tr><td>Malta</td><td>2016</td><td>-</td><td>-</td><td>-</td><td>-</td><td>-</td><td>-</td><td>-</td><td>-</td><td>-</td><td>-</td></tr>
<tr><td></td><td>2017</td><td>93</td><td>93</td><td>107</td><td>93</td><td>93</td><td>93</td><td>263</td><td>263</td><td>263</td><td>263</td></tr>
</table>

Country	Year	Amon	Ntri	Ntra	Phos	Tphs	Slca	Cphl	Temp	Psal	Doxy
	2018	165	165	186	165	165	165	480	481	481	473
	2019	59	59	66	59	59	59	78	77	77	77
	2020	-	-	-	-	-	-	-	-	-	-
	2021	-	-	-	-	-	-	-	-	-	-
Tunisia	2016-2021	No data provided									

Amon - Ammonium; Ntri- Nitrite; Ntra – Nitrate; Phos – Orthophosphate; Tphs—Total phosphorous; Slca – Orthosilicate; Cphl – Chlorophyll *a*; Temp – Temperature; Psal – Salinity; Doxy – Dissolved Oxygen.

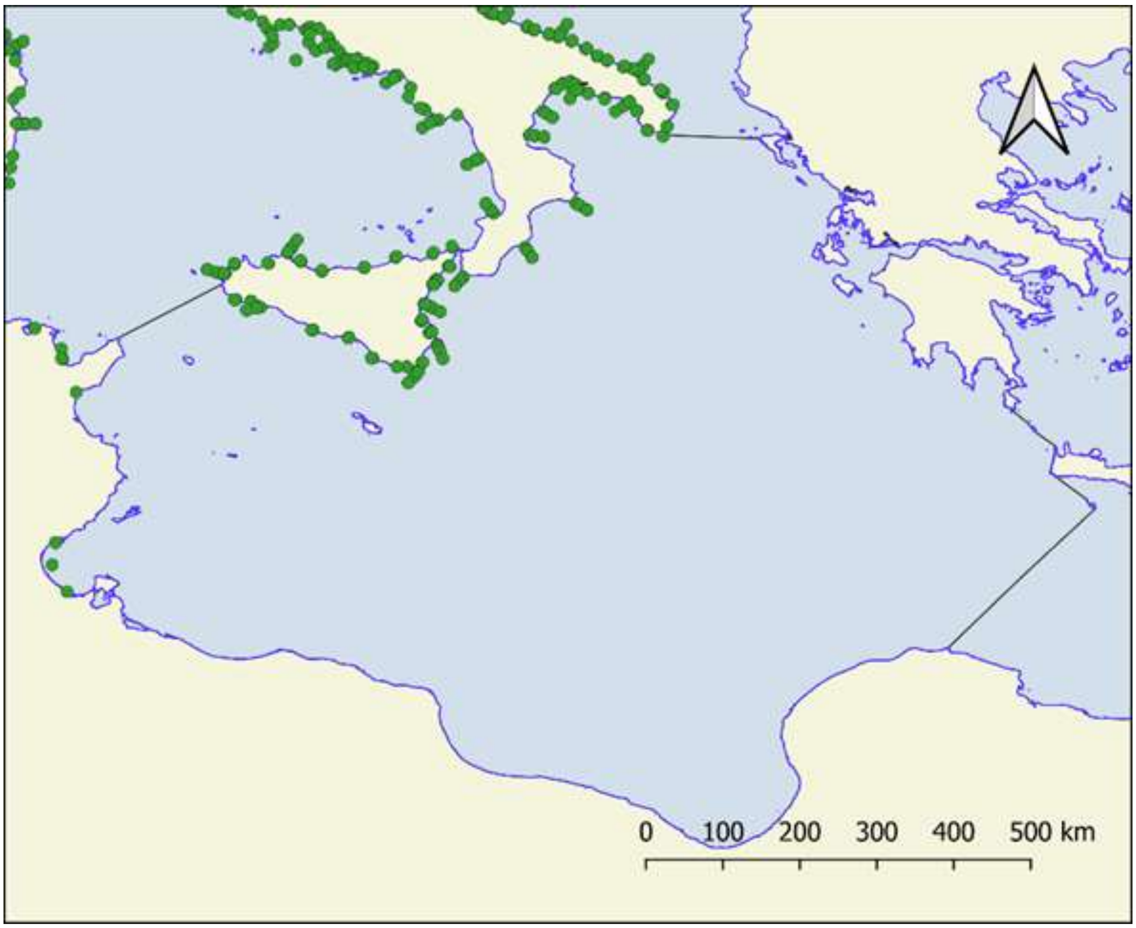

Figure 1. The locations of sampling stations in the CEN Sub-region

7. From Table 1 it can be found that the CPs in the southern Mediterranean rim did not report valid data as required by Decision IG.23/6 of COP 20 related to the 2017 Mediterranean Quality Status Report (MED QSR), and Decision IG.24/4 of COP21 providing the 2023 MED QSR Roadmap implementation.

8. Some of data were reported to IMAP IS very close to the 31st October, the cut-off date for data reporting, and without having a functional data quality control at the level of IMAP IS, at this late stage it was impossible to undertake data quality control and evaluation including through direct consultations with the CPs.

9. Given the above explained status of data reported, in particular lack of homogenous and quality assured data reported in line with IMAP requirements, it was necessary to explore the use of alternative data sources. The Copernicus source was found relevant regarding the existence of a systematic repository of remote sensing data for Chl *a*. Using only Chl *a* data, with a good geographical coverage (1 x 1 km)

and high sensing frequency (daily), it is possible to tentatively develop a simple assessment method, by applying ecological rules and a comparison of the obtained values to the defined G/M threshold. Due to a huge amount of data for the whole CEN, the data analysis process was very slow on an ordinary PC.

10. Chlorophyll *a* data for the CEN were downloaded from the Copernicus site (**OCEANCOLOUR_MED_BGC_L4_MY_009_144**).

11. For the Copernicus services the Mediterranean Sea Ocean Satellite Observations, the Italian National Research Council (CNR – Rome, Italy), elaborated the Bio-Geo_Chemical (BGC) regional datasets. Chlorophyll *a* concentration (CHL) were evaluated via region-specific algorithms (Case 1 waters: Volpe et al., 2019[1], with new coefficients; Case 2 waters, Berthon and Zibordi, 2004[2]), and the interpolated gap-free Chl concentration (to provide a "“cloud free”" product) was estimated by means of a modified version of the DINEOF algorithm (Volpe et al., 2018[3]).

12. The Copernicus product with ID: OCEANCOLOUR_MED_BGC_MY_009_144 was downloaded for the period from Jan 2016 to Dec 2021. It consists of Level 4 monthly values of Chlorophyll *a* concentration (CHL) with a resolution of 1 x 1 km. The file format is NetCDF-4 (.nc).

13. Data elaboration was performed by using R, an open-source language widely used for statistical analysis and graphical presentation (R Development Core Team, 2023)[4]. Maps are elaborated using QGIS 3.30, an open-source GIS tool. For the elaboration all relevant R Scripts are given in Annex I.

14. After download from the Copernicus site, as NetCDF file- .nc, the data were transferred to R data table using the *tidync* package. The transfer and data elaboration were very time demanding as the data set comprise **52 358 577 records**.

15. For every point of the grid (Figure 2), a geometric annual mean *(GM)* was calculated (Attila et al, 2018)[5]. The parameter values were expressed in µg/L of Chl *a*, for the *GM* calculated over the year in at least a five-year period as required in the COMMISSION DECISION (EU) 2018/229[6] . These *GM* annual values were later used as a metric for the development of the assessment criteria and present assessment of CI 14.

[1] Volpe, G., Colella, S., Brando, V. E., Forneris, V., Padula, F. L., Cicco, A. D., ... & Santoleri, R. (2019). Mediterranean ocean colour Level 3 operational multi-sensor processing. Ocean Science, 15(1), 127-146
[2] Berthon, J.-F., Zibordi, G. (2004) Bio-optical relationships for the northern Adriatic Sea. Int. J. Remote Sens., 25, 1527-1532.
[3] Volpe, G., Buongiorno Nardelli, B., Colella, S., Pisano, A. and Santoleri, R. (2018). An Operational Interpolated Ocean Colour Product in the Mediterranean Sea, in New Frontiers in Operational Oceanography, edited by E. P. Chassignet, A. Pascual, J. Tintorè, and J. Verron, pp. 227–244
[4] R Development Core Team (2023). R: A language and environment for statistical computing. R Foundation for Statistical Computing, Vienna, Austria. ISBN 3-900051-07-0. http://www.R-project.org
[5] Attila, J., Kauppila, P., Kallio, K.Y., Alasalmi, H., Keto, V., Bruun, E and Koponen, S. Applicability of Earth Observation chlorophyll-a data in assessment of water status via MERIS — With implications for the use of OLCI sensors. Remote Sensing of Environment 212 (2018) 273–287. https://doi.org/10.1016/j.rse.2018.02.043
[6] Commission Decision (EU) 2018/229 of 12 February 2018 establishing, pursuant to Directive 2000/60/EC of the European Parliament and of the Council, the values of the Member State monitoring system classifications as a result of the intercalibration.

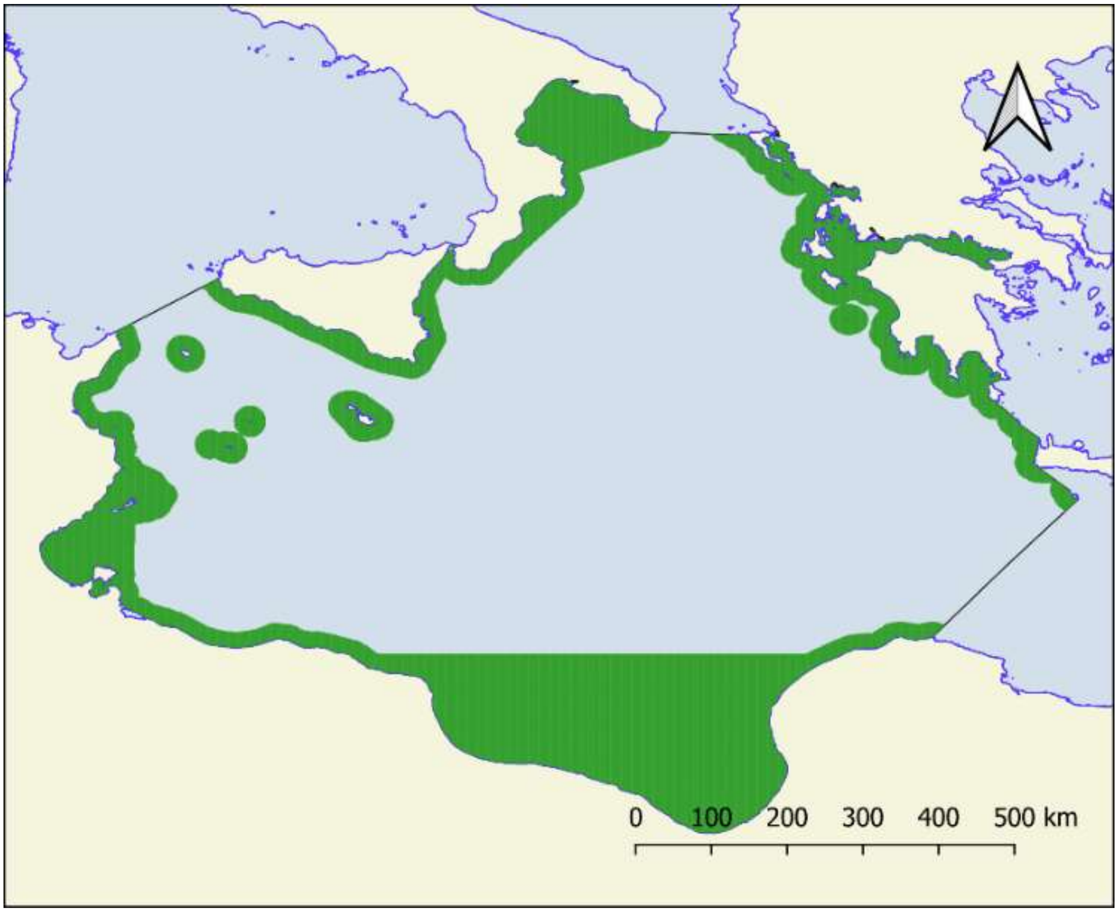

Figure 2. The CEN Sub-region: The dots in the assessment zones represent the data in the grid (1 x 1 km).

3. Setting of the areas of assessment

16. Following the rationale of the IMAP national monitoring programmes related to distribution of the monitoring stations, as well as the rules for integration and aggregation of the assessment products as elaborated in UNEP/MED WG.509/10/Rev.2, the two zones of assessment were defined in the CEN for the purposes of the present work: i) the coastal zone and ii) the offshore zone.

17. For purpose the of present work, it should also be recalled that GIS layers collected from different sources (International Hydrographic Organization – IHO Seas subdivisions, European Environment Information and Observation Network – EIONET (WFD delimitation (2018)); VLIZ marine subregions.

18. The principle of the NEAT IMAP assessment methodology applied in the Adriatic Sea Sub-region, as well as in the Western Mediterranean Sea Sub-region regarding CI 17, for setting of the spatial assessment units (SAUs) within the two main assessment zones along the IMAP nesting scheme, was also followed for setting of the coastal (CW) and the offshore monitoring zones (OW) in the CEN Sub-region. The CW included internal waters and one Nautical Mile outward. The offshore waters in the CEN start at the outward border of CW and extend to 20 km outward given this coverage corresponds to the area where national monitoring programmes are performed as shown in Figure 1.

19. Within the two Subdivisons i.e., the Central Mediterranean Sea and the Ionian Sea, the CW and OW AZs were divided in the four areas: Northern, Western, Eastern and Southern, which delimitations are shown on Figure 3 (upper map). It resulted in eight SAUs (i.e., CW_NCEN – Northern CW; OW_NCEN – Northern OW; CW_WCEN – Western CW; OW_WCEN – Western OW; CW_ECEN – Eastern CW; OW_ECEN – Eastern OW; Southern CW – CW_SCEN and Southern OW – OW_SCEN). The finest

IMAP subSAUs were further set on the base of nested assessment areas (AZs, four areas) by considering the national areas of monitoring and hydrographic characteristics.

20. The finest IMAP SAUs set in the CEN Sub-region for the purpose of the present CI 14 assessment are shown in Table 2. Figure 3 (lower map) depicts the finest IMAP SAUs nesting in the two main assessment zones i.e. CW and OW of the CEN Sub-region.

Table 2. The finest IMAP spatial assessment units (subSAUs)

Country	AZ	SAU	subSAU
GRE	CW	CW_ECEN	GREA
GRE	CW	CW_ECEN	GREAMB
GRE	CW	CW_ECEN	GREB
GRE	CW	CW_ECEN	GREC
GRE	CW	CW_ECEN	GRED
GRE	CW	CW_ECEN	GREISL
GRE	CW	CW_ECEN	GREKOR
GRE	CW	CW_ECEN	GREPAT
ITA	CW	CW_NCEN	ITAIOA
ITA	CW	CW_NCEN	ITAIOTAR
ITA	CW	CW_NCEN	ITASCA
ITA	CW	CW_NCEN	ITASCB
MLT	CW	CW_NCEN	MLTC
LBY	CW	CW_SCEN	LBY_E
LBY	CW	CW_SCEN	LBY_SIR
LBY	CW	CW_SCEN	LBY_W
TUN	CW	CW_WCEN	TUN_A
TUN	CW	CW_WCEN	TUN_B
GRE	OW	OW_ECEN	GREA
GRE	OW	OW_ECEN	GREB
GRE	OW	OW_ECEN	GREC
GRE	OW	OW_ECEN	GRED
GRE	OW	OW_ECEN	GREISL
ITA	OW	OW_NCEN	ITAIOA
ITA	OW	OW_NCEN	ITAIOTAR
ITA	OW	OW_NCEN	ITASCA
ITA	OW	OW_NCEN	ITASCAI
ITA	OW	OW_NCEN	ITASCB
MLT	OW	OW_NCEN	MLTC
LBY	OW	OW_SCEN	LBY_E
LBY	OW	OW_SCEN	LBY_SIR
LBY	OW	OW_SCEN	LBY_W
TUN	OW	OW_WCEN	TUN_A
TUN	OW	OW_WCEN	TUN_B

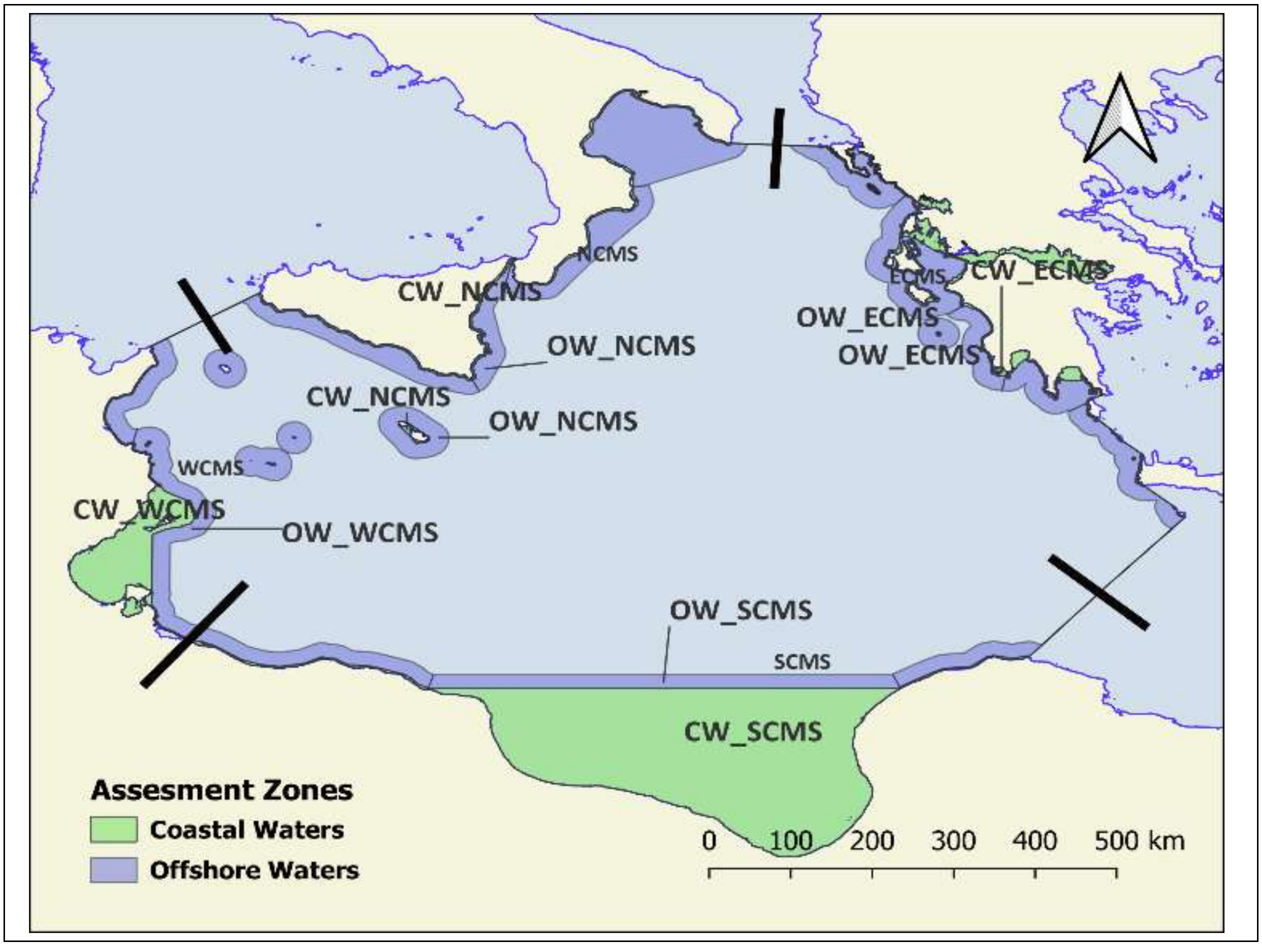
NCMS
CW_NCMS
OW_NCMS
CW_NCMS
OW_NCMS
WCMS
CW_WCMS
OW_WCMS
ECMS
CW_ECMS
OW_ECMS
OW_ECMS
OW_SCMS
SCMS
CW_SCMS
Assesment Zones
Coastal Waters
Offshore Waters
0 100 200 300 400 500 km

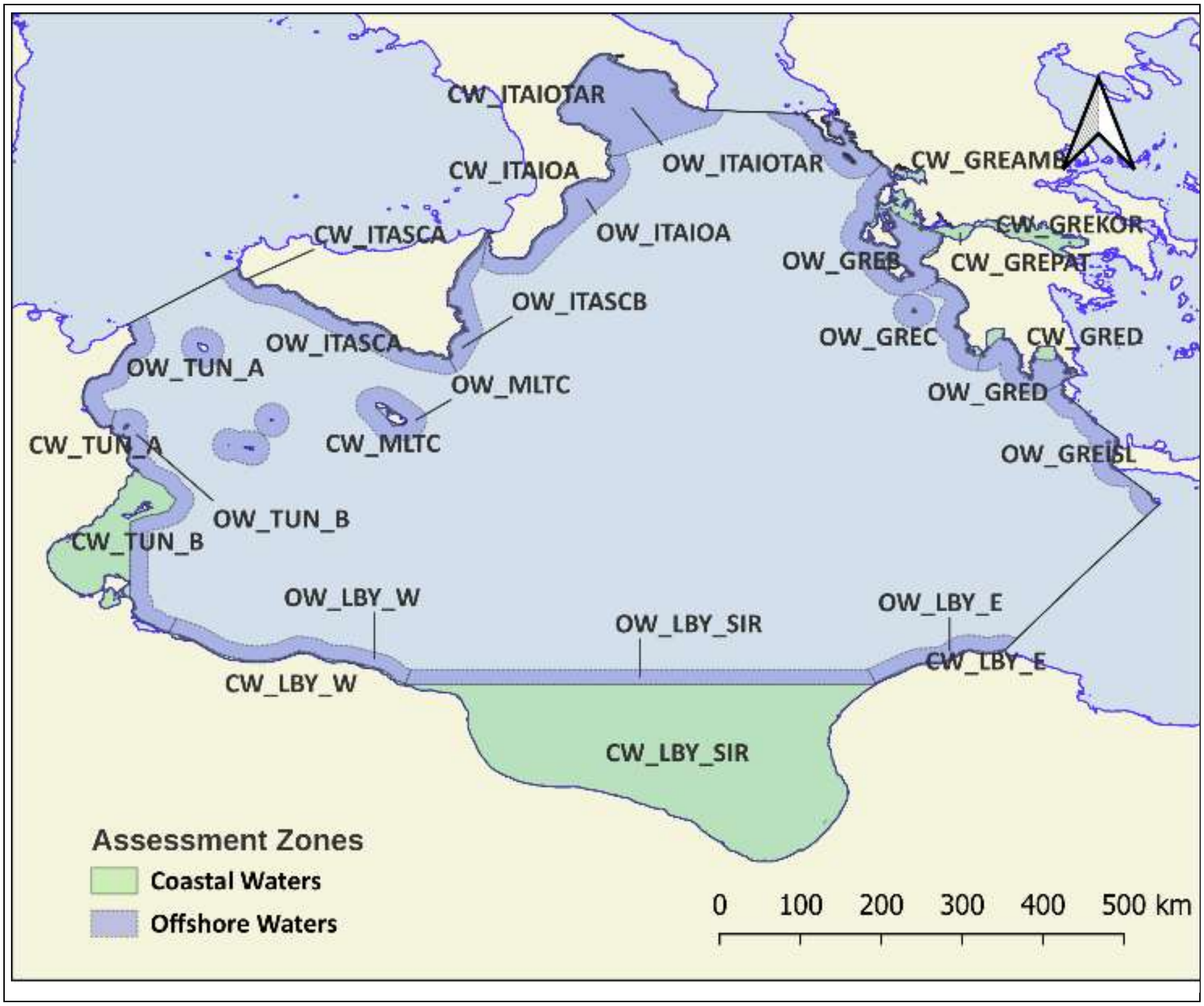

Figure 3. The nesting of IMAP SAUs set in the coastal (CW) and the offshore assessment (OW) zones for the CEN (upper map); and depiction of the finest IMAP subSAUs (lower map).

4. Setting the good/non good boundary value/threshold for the Simplified G/M comparison assessment methodology application in the CEN Sub-region.

21. The definition of baseline and threshold values for IMAP CIs 13 and 14 in the Mediterranean Sea is an ongoing process. Detail information on their present status is provided in UNEP/MED WG.533/10, Appendix II [7]. The setting of GES-nonGES boundary limits within the GES assessment of the Adriatic Sea Sub-region for IMAP CIs 13 and 14 were based on the boundary and reference values defined for TP and DIN, and updated ones for Chl *a*, as approved in UNEP/MED WG.533/10, Appendix II by the Meeting of CorMon on Pollution Monitoring (17 and 30 May 2022).

[7] UNEP/MED WG.533/10, Appendix II: Assessment Criteria. Assessment Criteria Methodologies for IMAP Common Indicator 13: Reference and Boundary Values for DIN and TP in the Adriatic Sea Sub-region, Meeting of the Ecosystem Approach Correspondence Group on Pollution Monitoring, videoconference, 27 and 30 May 2022., pp 59.

22. Within the present work, the attributes were added to all new satellite derived Chl *a* data points in order to allow their use for calculation of the assessment criteria by the CW and OW, and SAUs in the CEN Sub-region.

23. Namely, the use of a new parameter for assessment i.e. satellite derived Chl *a* imposes calculation of a new set of assessment criteria given absence of any tested relationship of the satellite derived Chl *a* data with *in situ* measured Chl *a* data based on effects-pressures relationship. Namely, the use of reference and boundary water types related values, as set by the Decision IG.23/6 of COP 20 (MED QSR), was impossible for the present work.

24. In order to calculate the assessment criteria applicable within the present work, the annual GM values for satellite derived Chl *a* data were normalized using the R package *bestNormalize*. Then, the normalization process was tested for usual normalisation transformation, log x, boxcox, yeojohnson and Ordered Quantile normalizing transformation (orderNorm). The best normalisation was obtained with *orderNorm()* as shown in Figure 4, and it was used for calculation of the assessment criteria applied to deliver the present CI 14 assessment.

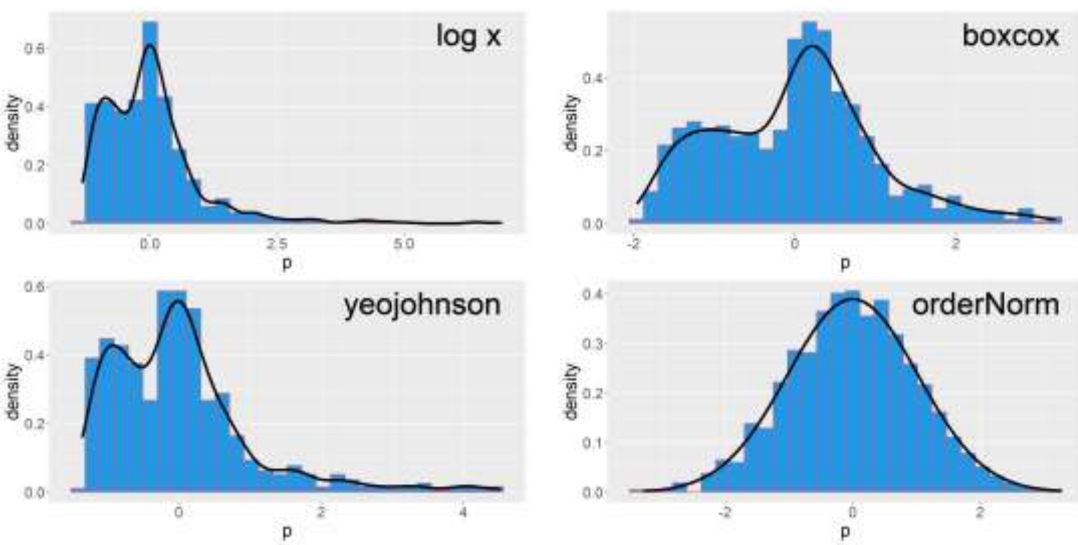

Figure 4. The distribution plot for various normalization transformation.

25. The Ordered Quantile (ORQ) normalization transformation, *orderNorm()*, is a rank-based procedure by which the values of a vector are mapped to their percentile, which is then mapped to the same percentile of the normal distribution. Without the presence of links to non-systematic processes, this essentially guarantees that the transformation leads to a uniform distribution.

26. The transformation is:

$$g(x) = \Phi^{-1}((rank(x) - .5)/(length(x)))$$

where Φ refers to the standard normal cdf, rank(x) refers to each observation's rank, and length(x) refers to the number of observations.

27. By itself, this method is certainly not new; the earliest mention of it is in a 1947 paper by Bartlett[8]. This equation was outlined explicitly in Van der Waerden (1952[9]), and expounded upon in Beasley (2009[10]).

28. Using linear interpolation between these percentiles, the ORQ normalization becomes a 1-1 transformation. This transformation can be performed on the satellite derived Chl*a* data and inverted via the *predict* function.

29. The normalization of data is important as it allows generation of the comparable datasets for different assessment zones within the specific Sub-region/Sub-division, and then at upper level between different Sub-regions/subdivision. Further to comparable datasets, it ensures calculation of all aspects relevant to data distribution i.e., z-scores, percentiles, means, etc.

30. The UNEP/MAP Guideline (UNEP(DEC)/MED WG.372/3[11]) defines reference conditions as the state of the marine environment (or a component) in which there is no disturbance or very minor disturbance from the pressures of human activities. Reference conditions (RC) may not necessarily reflect "background" or "historical" conditions, and it is up to the regulator to decide whether GES will represent pristine or slightly impacted but still "good" status (UNEP(DEC)/MED WG.372/3). For the present assessment of CI 14, the RC values were calculated from the normalized values and were represented by the 10th percentile.

31. Thresholds were used to define the boundary limit between the acceptable and the unacceptable environmental status i.e., the good/non good boundary value/threshold for the Simplified G/M comparison assessment methodology application in the CEN Sub-region. Further to the work undertaken in the Baltic Sea (Andersen et al. 201112; HELCOM 201013), for an indicator showing positive response (i.e., nutrients and Chl a), the threshold value has an upper limit of +50 % deviation from reference conditions. Setting the threshold to 50 % implies that low levels of disturbance (defined as less than +50 % deviation) resulting from human activity are considered acceptable, while moderate (i.e., greater than +50 %) deviations are not considered acceptable for the water body in question.

32. A further modification to this rule was applied within the present work in the CEN Sub-region given the 50th percentile represents the mean value of the distribution, and the 85th percentile ~ mean +1 SD represents the G/M threshold. It was necessary to use this criterion given expert-based analysis of the satellite derived Chl *a* preliminary indicates that most of the assessed waters are in the high status.

33. The transformation of percentile to z-scores were obtained using the *pnorm()* an *qnorm()* functions in R. The RC values (oN10) and the G/M thresholds (oN85) were calculated from the normalized values through the *predict* function. The results of calculation are presented in Table 3 and are obtained by the AZs and SAUs.

Table 3: Reference conditions (oN10) and G/M threshold (oN85) set by IMAP Assessment zones (AZ) and Spatial Assessment Units (SAU) in the CEN Sub-region.

AZ	SAU	CHL_N	oN50	oN50+50	oN90	oN10	oN85	oN25
CW	CW_ECEN	17376	0,147	0,221	0,351	0,06	0,264	0,081
CW	CW_NCEN	4618	0,329	0,493	0,957	0,102	0,78	0,182

[8] Bartlett, M. S. (1947) "The Use of Transformations." Biometrics, vol. 3, no. 1, pp. 39-52. JSTOR www.jstor.org/stable/3001536
[9] Van der Waerden BL. Order tests for the two-sample problem and their power. 1952;55:453-458. Ser A.
[10] Beasley TM, Erickson S, Allison DB (2009) Rank-based inverse normal transformations are increasingly used, but are they merited? Behav. Genet.; 39(5): 580-595. pmid:19526352
[11] UNEP(DEC)/MED WG.372/3 (2012) Approaches for definition of GES and setting targets for the pollution related ecological objectives in the framework of the ecosystem approach. (EO5: eutrophication, EP9: contaminants, EP10: marine litter, EO11: noise). Sarajevo, Bosnia and Herzegovina
[12] Andersen, J. H., Axe, P., Backer, H., Carstensen, J., Claussen, U., Fleming-Lehtinen, V., et al. (2011). Getting the measure of eutrophication in the Baltic Sea: towards improved assessment principles and methods. Biogeochemistry, 106(2), 137–156.
[13] HELCOM. (2010). Ecosystem health of the Baltic Sea 2003-2007: HELCOM Initial Holistic Assessment.

AZ	SAU	CHL_N	oN50	oN50+50	oN90	oN10	oN85	oN25
CW	CW_SCEN	298502	0,038	0,057	0,064	0,034	0,053	0,036
CW	CW_WCEN	41726	1,209	1,813	4,859	0,275	3,844	0,555
OW	OW_ECEN	98360	0,058	0,086	0,08	0,049	0,071	0,053
OW	OW_NCEN	152883	0,091	0,136	0,143	0,061	0,127	0,073
OW	OW_SCEN	80305	0,039	0,059	0,083	0,035	0,072	0,036
OW	OW_WCEN	46725	0,142	0,213	0,789	0,091	0,497	0,103
CHL_N – Number of calculated GM annual values, oN50 – Mean, oN50+50 – Mean + 50%, oN90 – 90^{th} percentile, oN10 – 10^{th} percentile, oN85 – 85^{th} percentile, oN25 – 25^{th} percentile								

34. Finally, each observation point, or area were classified in the good/non good status by comparing the value of the indicator to the class boundary between G/M i.e., the back transformed 85th percentile of normalized distribution.

35. It must be noted that by selecting the 85^{th} percentile of the normalized distribution as G/M boundary limit, therefore as the limit between the acceptable and the unacceptable statuses i.e. the good/non good status in the CEN Sub-region, the compatibility of the present classification was achieved with a five classes GES/non GES scale set in the Adriatic Sea Sub-region. The harmonization was achieved to the maximum possible extent given the Simplified assessment methodology based on G/M comparison and NEAT GES assessment methodology are different methodologies which application across the Mediterranean Sub-regions/Sub-divisions was conditioned with the statuses of data reported by the CPs. Therefore, the bias assessment of CI 14 within the 2023 MED QSR was avoided as the Simplified G/M method relay on the assessment criteria corresponding to RC and G/M as stated in the Decision 22/7 on Integrated Monitoring and Assessment Programme of the Mediterranean Sea and Coast and Related Assessment Criteria (UNEP/MAP, 2016). Based on statistical calculations and related selection of the 85^{th} percentile ~ mean +1 SD represents the G/M threshold, the synchronization was achieved to the maximal possible extent between the classification statuses assigned in the CEN Sub-region, and those in the Adriatic Sea Sub-region.

5. Results of the Assessment of CI 14 in the Central Mediterranean Sea Sub-region

36. The results of CI 14 assessment using the satellite derived Chl *a* data are presented in Tables 4 and 5, and Figure 6. The good status corresponds to the RC conditions, as well as to the values below the 85^{th} percentile of normalized distribution set as G/M i.e., good/non-good boundary limit (i.e. blue coloured cells in the last column of Tables 4 and 5). The non-good status corresponds to the class above G/M boundary limit (i.e. red coloured cells in the last column of Table 5). The assessment results show that all evaluated assessment zones can be considered likely in good status regarding assessment of the satellite derived Chl *a* data.

	GES			non-GES		
IMAP/NEAT	RC	High	Good	Moderate	Poor	Bad
Boundary limits and normalized NEAT scores	< RC/H limit, not in score scale	1 < score ≤ 0.8	0.8<score≤ 0.6	0.6<score ≤ 0.4	0.4< score ≤0.2	Score<0.2
IMAP/Simplified G/M						
Boundary limits*	≤10^{th} %	>10^{th}% CHL_GM ≤85^{th}%		CHL_GM >85^{th} %		
G/NG threshold			**G/M**			
*** Percentile are calculated from normalized (with Ordered Quantile transformation) annual geometric mean (for at list 5 year)**						

Figure 5: Assessment classification for harmonized IMAP/NEAT and IMAP/Simplified G/M assessment methodologies application in the Mediterannean Sea Sub-regions.

37. The assessment results show that all evaluated assessment zones can be considered likely in good status regarding the assessment of the satellite-derived Chl *a* data. Further to this good status assigned to the assessment zones, it can be preliminarily found that 7 out of 36 subSAUs is likely in non-good status. However, it must be noted that the subSAUs are set at an insufficient level of fineness for a reliable assessment (Tables 4 and 5, and Figure 6). The subSAUs in non-good status (GREA, GREAMB, GREPAT, LBY_E, LBY_W, LBY_W; TUN_B) are in the Eastern and Southern parts of the CEN Sub-region.

38. The subSAU GREAMB is located in Ambracian Gulf and subSAU GREPAT in Gulf of Patras, and are mainly related to agriculture (Pavlidou et al., 2015) and Gulf of Patras (GREPAT) sites , with pressures that include harbor operations, industries and agriculture (Pavlidou et al., 2015)[14].These sites were also classified as moderate or a poor status by Greek research studies[15]. In subSAU GREAMB, the highest *GM* value of Chl *a* was observed (4,8 µg/L; Table 5). The Northern subSAU GREA is probably influenced by the local sources of pollution (Igumenitsa port and intense aquaculture, (Pavlidou et al., 2015)). The level of the finesse of the subSAU definition contributes to the lower confidence of the assessment findings, i.e., the assessment of the larger area is less confident. A finer-designed approach will contribute to a more accurate assessment of the local processes, contributing to the understanding of the very localized problem.

39. Along the coast of Libya, the marine waters impacted by eutrophication are located in the western part of Libyan OW (subSAU LBYW) and in the eastern part of CW (subSAU LBYE). It must be noticed that the G/M threshold for the Libyian waters is very low which questions the evaluation of the Southern part of the CEN Sub-region. The western part of the coast of Libya is influenced by the waters coming from the Gulf of Gabes where human activities contribute to the impacts of eutrophication.[16] Many pressures that could cause impacts of eutrophication are present in the Gulf: i) large urban center, ii) untreated domestic discharges, iii) industrial discharges, among them phosphogypsum, iv) agrochemical industry. v) agriculture. The local influence of Tripoli should also be taken into account.

40. Further to calculations undertaken for the Gulf of Gabes, the subSAU TUNB located in CW can be indicated as an area in good status. However, it must be recognized that using the 50^{th} percentile for the development of the assessment criteria is not applicable in heavily impacted areas, such as the Gulf of Gabes. Therefore, an adjustment by using the 25^{th} percentile of the calculated values resulted in the classification of the subSAU TUNB in non-good status, as also recognized in the existing literature.

Table 4. Results of the assessment (G_NG.oN85 - the good status class corresponding to all values below the 85th percentile set as G/M i.e., good/non-good boundary limit) of the CEN Sub-region by Assessment Zones (AZ) and Spatial Assessment Units (SAUs). Blue coloured SAUs indicate good status.

AZ	**SAU**	**CHL_N**	**CHL_GM**	**oN50**	**oN50+50**	**oN10**	**oN85**	**G_NG.oN85**

[14] Pavlidou, A., N. Simboura, E. Rousselaki, M. Tsapakis, K. Pagou, P. Drakopoulou, G. Assimakopoulou, H. Kontoyiannis and P. Panayotidis (2015). "Methods of eutrophication assessment in the context of the water framework directive: Examples from the Eastern Mediterranean coastal areas." Continental Shelf Research 108: 156-168.
[15] Simboura et al. (2015) Assessment of the environmental status in the Hellenic coastal waters (Eastern Mediterranean): from the Water Framework Directive to the Marine Strategy Framework Directive. Medit. Mar. Sci., 16/1, 46-64
[16] Annabi-Trabelsi, N., Guermazi, W., Leignel, V., Al-Enezi, Y., Karam, Q., Ali Mohammad Ayadi, H., Belmonte, G. (2022). Effects of Eutrophication on Plankton Abundance and Composition in the Gulf of Gabès (Mediterranean Sea, Tunisia). Water. 14. 2230. 10.3390/w14142230.

CW	CW_ECEN	26254	0,174	0,147	0,221	0,060	0,264	**G**
CW	CW_NCEN	8893	0,330	0,329	0,493	0,102	0,78	**G**
CW	CW_SCEN	300536	0,045	0,038	0,057	0,034	0,053	**G**
CW	CW_WCEN	44184	1,297	1,209	1,813	0,275	3,844	**G**
OW	OW_ECEN	99313	0,061	0,058	0,086	0,049	0,071	**G**
OW	OW_NCEN	154096	0,094	0,091	0,136	0,061	0,127	**G**
OW	OW_SCEN	80305	0,049	0,039	0,059	0,035	0,072	**G**
OW	OW_WCEN	46845	0,198	0,142	0,213	0,091	0,497	**G**
CHL_N – number of grid point in the SAU; CHL_GM – geometric mean (5-year average); oN50 – mean; oN50+50 – Mean + 50%; oN10 – 10th percentile (Reference conditions)								

Table 5. Result of the assessment (G_NG.oN85- the good status class corresponding to all values below the 85th percentile set as G/M i.e., good/non-good boundary limit) of the CEN Sub-region for the finest Spatial Assessment Units (subSAUs). Blue coloured subSAUs indicate good status; Red coloured status indicate non-good status.

Coun.	AZ	SAU	subSAU	CHL_N	CHL_GM	oN50+50	oN10	oN85	G_NG.oN85
GRE	CW	CW_ECEN	GREA	1702	0,167	0,221	0,06	0,264	G
GRE	CW	CW_ECEN	GREAMB	1303	4,8	0,221	0,06	0,264	NG
GRE	CW	CW_ECEN	GREB	6773	0,122	0,221	0,06	0,264	G
GRE	CW	CW_ECEN	GREC	1214	0,129	0,221	0,06	0,264	G
GRE	CW	CW_ECEN	GRED	3753	0,091	0,221	0,06	0,264	G
GRE	CW	CW_ECEN	GREISL	998	0,056	0,221	0,06	0,264	G
GRE	CW	CW_ECEN	GREKOR	8157	0,191	0,221	0,06	0,264	G
GRE	CW	CW_ECEN	GREPAT	2354	0,31	0,221	0,06	0,264	NG
ITA	CW	CW_NCEN	ITAIOA	1421	0,227	0,493	0,102	0,78	G
ITA	CW	CW_NCEN	ITAIOTAR	2630	0,382	0,493	0,102	0,78	G
ITA	CW	CW_NCEN	ITASCA	2784	0,615	0,493	0,102	0,78	G
ITA	CW	CW_NCEN	ITASCB	1535	0,198	0,493	0,102	0,78	G
MLT	CW	CW_NCEN	MLTC	523	0,071	0,493	0,102	0,78	G
LBY	CW	CW_SCEN	LBY_E	1170	0,097	0,057	0,034	0,053	NG
LBY	CW	CW_SCEN	LBY_SIR	296417	0,044	0,057	0,034	0,053	G
LBY	CW	CW_SCEN	LBY_W	2949	0,348	0,057	0,034	0,053	NG
TUN	CW	CW_WCEN	TUN_A	995	0,431	1,813	0,275	3,844	G
TUN	CW	CW_WCEN	TUN_B	43189	1,33	1,813	0,275	3,844	NG
GRE	OW	OW_ECEN	GREA	16138	0,076	0,086	0,049	0,071	NG
GRE	OW	OW_ECEN	GREB	32001	0,068	0,086	0,049	0,071	G
GRE	OW	OW_ECEN	GREC	18781	0,056	0,086	0,049	0,071	G
GRE	OW	OW_ECEN	GRED	14808	0,055	0,086	0,049	0,071	G
GRE	OW	OW_ECEN	GREISL	17585	0,05	0,086	0,049	0,071	G
ITA	OW	OW_NCEN	ITAIOA	23686	0,092	0,136	0,061	0,127	G
ITA	OW	OW_NCEN	ITAIOTAR	53598	0,114	0,136	0,061	0,127	G
ITA	OW	OW_NCEN	ITASCA	25605	0,112	0,136	0,061	0,127	G
ITA	OW	OW_NCEN	ITASCAI	22978	0,07	0,136	0,061	0,127	G
ITA	OW	OW_NCEN	ITASCB	13608	0,095	0,136	0,061	0,127	G
MLT	OW	OW_NCEN	MLTC	14621	0,057	0,136	0,061	0,127	G
LBY	OW	OW_SCEN	LBY_E	13675	0,04	0,059	0,035	0,072	G

Coun.	AZ	SAU	subSAU	CHL_N	CHL_GM	oN50+50	oN10	oN85	G_NG.oN85
LBY	OW	OW_SCEN	LBY_SIR	43480	0,038	0,059	0,035	0,072	G
LBY	OW	OW_SCEN	LBY_W	23150	0,089	0,059	0,035	0,072	NG
TUN	OW	OW_WCEN	TUN_A	14645	0,11	0,213	0,091	0,497	G
TUN	OW	OW_WCEN	TUN_B	32200	0,258	0,213	0,091	0,497	G
CHL_N – number of grid point in the SAU; CHL_GM – geometric mean (5 year average); oN50 – mean; oN50+50 – Mean + 50%; oN10 – 10th percentile (Reference conditions);									

6. Conclusions and Key Findings

41. The results of the CI 14 assessment provided by the application of the Simplified assessment methodology based on G/M comparison by using the Copernicus satellite-derived Chl *a* data are shown by the respective colours in Figure 6.

42. The maps depict the acceptable and non-acceptable statuses i.e. good/non-good status assigned at the level of SAUs set in the CEN Sub-region.

43. As explained above, the good status corresponds to the RC conditions class (column oN10 in Tables 4 and 5), as well as to the class between the RC and G/M boundary limit, set as the back-transformed 85th percentile of normalized distribution (i.e. blue coloured cells in the last column of Tables 4 and 5), which is depicted in blue coloured subSAUs in Figure 6. The non-good status corresponds to the class above G/M boundary limit (i.e., red coloured cell in the last G_NG.oN85 column of Table 5) which is depicted in red coloured subSAUs in Figure 6.

44. Further to the good status assigned to the assessment zones, it can be preliminarily found that 7 out of 36 subSAUs is in non-good status. However, it must be noted that the subSAUs are set at an insufficient level of fineness for a reliable assessment (Tables 4 and 5, and Figure 6). The subSAUs in non-good status (GREA, GREAMB, GREPAT, LBY_E, LBY_W, LBY_W; TUN_B) are in the Eastern and Southern parts of the CEN Sub-region.

45. The Golf of Gabes (TUNB) was classified in the good status, and it must be stated that probably the applied criteria to use the mean as the starting condition for the development of the assessment criteria is not applicable in heavily impacted area as is the Gulf. Probably a better criterion will be to use the 25th percentile for the calculus. If we apply that criterion the subSAU TUNB will be in non-good status as is to be expected. Anyway, in future the approach must be enhanced to give reliable results.

46. The subSAU GREAMB is located in Ambracian Gulf and subSAU GREPAT in Gulf of Patras. The Northern subSAU GREA is probably influenced by the local sources of pollution (Igumenitsa port and intense aquaculture). The level of finesse of the subSAU definition contributes to the lower confidence of the assessment findings, i.e., the assessment of the larger area is less confident. A finer-designed approach will contribute to a more accurate assessment of the local processes, contributing to the understanding of the very localized problem.

47. Along the coast of Libya, the marine waters impacted by eutrophication are located in the western part of Libyan OW (subSAU LBYW) and in the eastern part of CW (subSAU LBYE). The western part of the coast of Libya is influenced by the waters coming from the Gulf of Gabes where human activities contribute to the impacts of eutrophication. The local influence of Tripoli should also be taken into account.

48. Further to the application of the 25th percentile for the development of the assessment criteria in heavily impacted areas, the subSAU TUNB was classified in non-good status, as also recognized in the existing literature.

49. The results of the present CI 14 assessment in the Central Mediterranean Sea Sub-region represent only an indication of possible good/non good status at the level of the subSAUs, whereby they are not set at the same level of spatial finesse. Namely, the reliability of the assessment was negatively affected by the lack of data reported by the CPs in IMAP IS, and therefore impossibility to use the IMAP NEAT GES assessment as applied to the Adriatic Sea Sub-region.

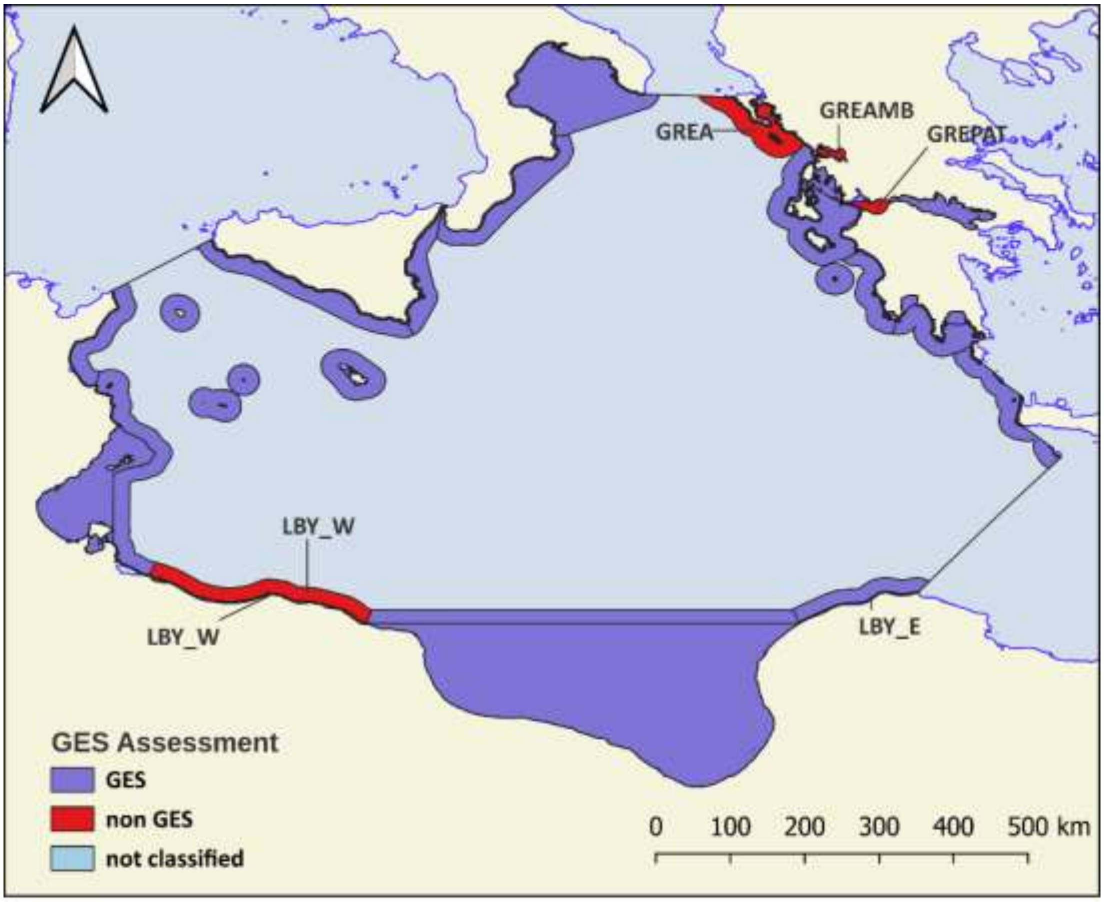

Figure 6: The assessment results for CI 14 in the CEN Sub-region by applying the simplified G/M method at the level of subSAUs.

Annex I
R scripts

Four R script used for the data conversion, calculation of statistical central tendency measures, normalization of data and the calculation of assessment criteria are listed.

R1 – data conversion

```
library(ncdf4)
library(RNetCDF)
library(tidync)
library(dplyr)
library(plyr)
library(lubridate)
library(data.table)

nc = "Data\\LEV\\Levantine_Ocli_16-21.nc"

#Conversion of nc to data.table

dft <- tidync(nc) %>%
    hyper_tibble()

dft <- mutate(dft, Month=month(as.Date(as.POSIXct(time, origin="1981-01-01"))))
dft <- mutate(dft, Year=year(as.Date(as.POSIXct(time, origin="1981-01-01"))))
dft <- dft[, c(8,7,4,5,1,2,3)]
dft <- dft[!is.na(dft$CHL),]
write.csv(dft,"Data\\ALB\\ALB_Chla_16_21_F.csv", row.names = FALSE)

save(dft, file = "Data\\LEV\\LEV_Chla_16_21_F.RData")
View(dft)
```

R2 – calculations

```
# Load libraries ----
library(readr)
library(readxl)
library(dplyr)
library(openxlsx)
library(plotrix)
library(EnvStats)
library(bestNormalize)
library(ggplot2)
library(ggpp)

# Get data ----
load("Data/Levantine/LEV_Chla_16_21_F.RData")


# Stat CHL YLL ----
LEV_S1 <- dft %>%
  group_by(Year, lon, lat) %>%
  summarize(CHL_N = n(),
           CHL_GM = round(geoMean(CHL, na.rm = TRUE),3),
           CHL_Mean = round(mean(CHL, na.rm = TRUE),3),
           CHL_Med = round(median(CHL, na.rm = TRUE),3),
           CHL_p90 = round(quantile(CHL, na.rm = TRUE, probs = 0.90),3),
           CHL_SD = round(sd(CHL, na.rm = TRUE),3),
           CHL_SE = round(std.error(CHL, na.rm = TRUE),3))

# Stat CHL LL ----
LEV_S2 <- dft %>%
  group_by(lon, lat) %>%
  summarize(CHL_N = n(),
           CHL_GM = round(geoMean(CHL, na.rm = TRUE),3),
           CHL_Mean = round(mean(CHL, na.rm = TRUE),3),
           CHL_Med = round(median(CHL, na.rm = TRUE),3),
           CHL_p90 = round(quantile(CHL, na.rm = TRUE, probs = 0.90),3),
           CHL_SD = round(sd(CHL, na.rm = TRUE),3),
           CHL_SE = round(std.error(CHL, na.rm = TRUE),3))

write.csv(LEV_S1,file='Data/LEV_Chla_16_21_1.csv')
write.csv(LEV_S2,file='Data/LEV_Chla_16_21_2.csv')
```

R3 – Normalization and assessment criteria

```
# Load libraries ----
library(readr)
library(readxl)
library(dplyr)
library(openxlsx)
library(plotrix)
library(EnvStats)
library(bestNormalize)
library(ggplot2)
library(ggpp)

# Get data ----
f <- read_delim("Data/Levantine/LEV_Chla_16_21_1_F.csv",
                    delim = ",", escape_double = FALSE, trim_ws = TRUE)
f <- subset(f, (CHL_N > 5))

# Stat CHL_GM----
ALB_S10 <- f %>%
  group_by(AZ, SAU1) %>%
  summarize(CHL_N = n(),
        oN50 = round(predict(orderNorm(CHL_GM), newdata = 0, inverse = TRUE) ,3),
        oN51 = round(predict(orderNorm(CHL_GM), newdata = 0, inverse = TRUE)*1.5, 3),
        oN90 = round(predict(orderNorm(CHL_GM), newdata = 1.282, inverse = TRUE), 3),
        oN10 = round(predict(orderNorm(CHL_GM), newdata = -1.282, inverse = TRUE), 3),
        oN85 = round(predict(orderNorm(CHL_GM), newdata = 1, inverse = TRUE), 3),
        oN25 = round(predict(orderNorm(CHL_GM), newdata = -0.674, inverse = TRUE), 3))

# Stat CHL_p90 ----
ALB_S11 <- f %>%
  group_by(AZ, SAU1) %>%
  summarize(CHL_N = n(),
        oN50 = round(predict(orderNorm(CHL_p90), newdata = 0, inverse = TRUE) ,3),
        oN51 = round(predict(orderNorm(CHL_p90), newdata = 0, inverse = TRUE)*1.5, 3),
        oN90 = round(predict(orderNorm(CHL_p90), newdata = 1.282, inverse = TRUE), 3),
        oN10 = round(predict(orderNorm(CHL_p90), newdata = -1.282, inverse = TRUE), 3),
        oN85 = round(predict(orderNorm(CHL_p90), newdata = 1, inverse = TRUE), 3),
        oN25 = round(predict(orderNorm(CHL_p90), newdata = -0.674, inverse = TRUE), 3))


#T01_GM orderNorm ----
x <- subset(f, ((AZ=="CW") & (SAU1=="NO")),
        select=c(AZ, SAU1, lon, lat, CHL_GM, CHL_p90, CHL_N))

oN_obj <- orderNorm(x$CHL_GM)
oN_obj
p <- predict (oN_obj)
p = as.data.frame(p)

ggplot(p, aes(x=p))+geom_histogram(aes(y = ..density..), bins = 30, col=2, fill=4)+
    geom_line(stat = "density", linewidth = 1.5)+
    geom_text_npc(aes(npcx = "right", npcy = "top", label = "orderNorm"), size=12)+
    theme(text = element_text(size = 20))
```

```
ggsave("Outputs/CW_NO_oN.png")

oN50 <- round(predict(orderNorm(x$CHL_GM), newdata = 0, inverse = TRUE),3)
oN50
oN51 <- predict(oN_obj, newdata = oN50*1.5, inverse = FALSE)
oN51
oN90 <- predict(oN_obj, newdata = 1.282, inverse = TRUE)
oN90
oN92 <- predict(oN_obj, newdata = -1.282, inverse = TRUE)
oN92
oN93 <- predict(oN_obj, newdata = 1, inverse = TRUE)
oN93
oN94 <- predict(oN_obj, newdata = -0.674, inverse = TRUE)
oN94

#T01_GM yeojohnson ----
yN_obj <- yeojohnson(x$CHL_GM)
yN_obj
p <- predict (yN_obj)
p = as.data.frame(p)

ggplot(p, aes(x=p))+geom_histogram(aes(y = ..density..), bins = 30, col=2, fill=4)+
    geom_line(stat = "density", linewidth = 1.5)+
    geom_text_npc(aes(npcx = "right", npcy = "top", label = "yeojohnson"), size=12)+
    theme(text = element_text(size = 20))

ggsave("Outputs/CW_NO_yN.png")

yN50 <- predict(yN_obj, newdata = 0, inverse = TRUE)
yN50
yN51 <- predict(yN_obj, newdata = yN50*1.5, inverse = FALSE)
yN51
yN90 <- predict(yN_obj, newdata = 1.282, inverse = TRUE)
yN90
yN92 <- predict(yN_obj, newdata = -1.282, inverse = TRUE)
yN92
yN93 <- predict(yN_obj, newdata = 1, inverse = TRUE)
yN93

#T01_GM boxcox ----
bc_obj <- boxcox(x$CHL_GM)
bc_obj
p <- predict (bc_obj)
p = as.data.frame(p)

ggplot(p, aes(x=p))+geom_histogram(aes(y = ..density..), bins = 30, col=2, fill=4)+
    geom_line(stat = "density", linewidth = 1.5)+
    geom_text_npc(aes(npcx = "right", npcy = "top", label = "boxcox"), size=12)+
    theme(text = element_text(size = 20))

ggsave("Outputs/CW_NO_bc.png")

bc50 <- predict(bc_obj, newdata = 0, inverse = TRUE)
bc50
bc51 <- predict(bc_obj, newdata = bc50*1.5, inverse = FALSE)
bc51
```

```
bc90 <- predict(bc_obj, newdata = 1.282, inverse = TRUE)
bc90
bc92 <- predict(bc_obj, newdata = -1.282, inverse = TRUE)
bc92
bc93 <- predict(bc_obj, newdata = 1, inverse = TRUE)
bc93

#T01_GM logx ----
lx_obj <- log_x(x$CHL_GM)
lx_obj
p <- predict (lx_obj)
p = as.data.frame(p)

ggplot(p, aes(x=p))+geom_histogram(aes(y = ..density..), bins = 30, col=2, fill=4)+
  geom_line(stat = "density", linewidth = 1.5)+
  geom_text_npc(aes(npcx = "right", npcy = "top", label = "log x"), size=12)+
  theme(text = element_text(size = 20))

ggsave("Outputs/CW_NO_lx.png")

lx50 <- predict(lx_obj, newdata = 0, inverse = TRUE)
lx50
lx51 <- predict(lx_obj, newdata = lx50*1.5, inverse = FALSE)
lx51
lx90 <- predict(lx_obj, newdata = 1.282, inverse = TRUE)
lx90
lx92 <- predict(lx_obj, newdata = -1.282, inverse = TRUE)
lx92
lx93 <- predict(lx_obj, newdata = 1, inverse = TRUE)
lx93

# HeaderStyles ----
hs_RP <- createStyle(fgFill = "#4F81BD", halign = "CENTER",
                     textDecoration = "Bold",border = "Bottom",
                     fontColour = "white")

#Save as xls ----
l<- list("Cphl_GM" = ALB_S10, "Cphl_p90" = ALB_S11)
write.xlsx(l, "Outputs/Levantine.xlsx", firstRow = TRUE,
           colWidths =  "auto",  headerStyle = hs_RP )
```

R4 – Assessment

```
# Load libraries ----
library(readr)
library(readxl)
library(dplyr)
library(openxlsx)
library(plotrix)
library(EnvStats)
library(bestNormalize)
library(ggplot2)
library(ggpp)

# Get data ----
f <- read_delim("Data/Levantine/LEV_Chla_16_21_2_F.csv",
                                  delim = ",", escape_double = FALSE, trim_ws = TRUE)
f <- subset(f, (CHL_N > 24))

# Stat CHL_GM ISO_SOV1, AZ----
ALB_S70 <- f %>%
  group_by(AZ, SAU1) %>%
  summarize(CHL_N = n(),
            CHL_GM1 = round(geoMean(CHL_GM, na.rm = TRUE),3),
            CHL_Mean = round(mean(CHL_GM, na.rm = TRUE),3),
            CHL_Med = round(median(CHL_GM, na.rm = TRUE),3),
            CHL_p90 = round(quantile(CHL_GM, na.rm = TRUE, probs = 0.90),3),
            CHL_SD = round(sd(CHL_GM, na.rm = TRUE),3),
            CHL_SE = round(std.error(CHL_GM, na.rm = TRUE),3))

# Stat CHL_GM ISO_SOV1, AZ, localId----
ALB_S71 <- f %>%
  group_by(AZ, SAU1, SAU2) %>%
  summarize(CHL_N = n(),
            CHL_GM1 = round(geoMean(CHL_GM, na.rm = TRUE),3),
            CHL_Mean = round(mean(CHL_GM, na.rm = TRUE),3),
            CHL_Med = round(median(CHL_GM, na.rm = TRUE),3),
            CHL_p90 = round(quantile(CHL_GM, na.rm = TRUE, probs = 0.90),3),
            CHL_SD = round(sd(CHL_GM, na.rm = TRUE),3),
            CHL_SE = round(std.error(CHL_GM, na.rm = TRUE),3))

ALB_S72 <- left_join(ALB_S70, ALB_S10, by = c("AZ", "SAU1"))
ALB_S72 <-  mutate(ALB_S72, G_NG51 = ifelse(oN51 > CHL_GM1,"G","NG"))
ALB_S72 <-  mutate(ALB_S72, G_NG85 = ifelse(oN85 > CHL_GM1,"G","NG"))
ALB_S72 <-  mutate(ALB_S72, CO_WT = paste(AZ,SAU1,sep = "" ))
write.csv(ALB_S72,"Data/Levantine/ALB_S72.csv", row.names = FALSE)

ALB_S73 <- left_join(ALB_S71, ALB_S10, by = c("AZ", "SAU1"))
ALB_S73 <-  mutate(ALB_S73, G_NG51 = ifelse(oN51 > CHL_GM1,"G","NG"))
ALB_S73 <-  mutate(ALB_S73, G_NG85 = ifelse(oN85 > CHL_GM1,"G","NG"))
ALB_S73 <-  mutate(ALB_S73, CO_WT = paste(AZ,SAU1,sep = ""))
ALB_S73 <-  mutate(ALB_S73, CO_WT_WF = paste(AZ,SAU1,SAU2,sep = ""))
write.csv(ALB_S73,"Data/Levantine/ALB_S73.csv", row.names = FALSE)

ALB_S74 <- left_join(f, ALB_S10, by = c("AZ", "SAU1"))
ALB_S74 <-  mutate(ALB_S74, G_NG51 = ifelse(oN51 > CHL_GM,"G","NG"))
ALB_S74 <-  mutate(ALB_S74, G_NG85 = ifelse(oN85 > CHL_GM,"G","NG"))
```

```
ALB_S74 <-  mutate(ALB_S74, RC = ifelse(oN10 < CHL_GM,"RC","NRC"))
ALB_S74 <-  mutate(ALB_S74, CO_WT = paste(AZ,SAU1,sep = ""))
ALB_S74 <-  mutate(ALB_S74, CO_WT_WF = paste(AZ,SAU1,SAU2,sep = ""))
write.csv(ALB_S74,"Data/Levantine/ALB_S74.csv", row.names = FALSE)

# HeaderStyles ----
hs_RP <- createStyle(fgFill = "#4F81BD", halign = "CENTER",
                     textDecoration = "Bold",border = "Bottom",
                     fontColour = "white")

#Save as xls ----
l<- list("Cphl_GM-2" = ALB_S70, "Cphl_GM-3" = ALB_S71)
write.xlsx(l, "Outputs/Levantine_23.xlsx", firstRow = TRUE,
          colWidths =  "auto",  headerStyle = hs_RP )

l<- list("Cphl_GM_G_NG_2" = ALB_S72, "Cphl_GM_G_NG_3" = ALB_S73)
write.xlsx(l, "Outputs/Levantine_45.xlsx", firstRow = TRUE,
          colWidths =  "auto",  headerStyle = hs_RP )
```

Annex II
Reference

UNEP(DEC)/MED WG.372/3 (2012) Approaches for definition of GES and setting targets for the pollution related ecological objectives in the framework of the ecosystem approach. (EO5: eutrophication, EP9: contaminants, EP10: marine litter, EO11: noise). Sarajevo, Bosnia and Herzegovina

UNEP/MAP (2016). Decision 22/7 on Integrated Monitoring and Assessment Programme of the Mediterranean Sea and Coast and Related Assessment Criteria" (COP18).

UNEP/MAP (2019). UNEP/MED WG.463/8. Approaches on Scales of Monitoring for Common Indicators related to pollution

UNEP/MAP (2021). UNEP/MED WG.509/10//Rev.2 Integration and Aggregation Rules for Monitoring and Assessment of (IMAP Pollution and Marine Litter Cluster)

UNEP/MAP (2022). UNEP/MED WG.533/10, Appendix II: Assessment Criteria. Assessment Criteria Methodologies for IMAP Common Indicator 13: Reference and Boundary Values for DIN and TP in the Adriatic Sea Sub-region, Meeting of the Ecosystem Approach Correspondence Group on Pollution Monitoring, Videoconference, 27 and 30 May 2022., pp 59.

UNEP/MED WG.533/Inf.5/Rev.1 (2022): The GIS -based Layers for the Finest Areas of Assessment and the Areas of Assessment Nested to the Levels of Integration that are Considered Meaningful for Their Use Within NEAT Tool Application for the GES Assessment of the IMAP Common Indicator 17 of Ecological Objective 9, as well as for the Assessments related to Ecological Objectives 5 and 10

Annabi-Trabelsi, N., Guermazi, W., Leignel, V., Al-Enezi, Y., Karam, Q., Ali Mohammad Ayadi, H., Belmonte, G. (2022). Effects of Eutrophication on Plankton Abundance and Composition in the Gulf of Gabès (Mediterranean Sea, Tunisia). Water. 14. 2230. 10.3390/w14142230.

Andersen, J. H., Axe, P., Backer, H., Carstensen, J., Claussen, U., Fleming-Lehtinen, V., et al. (2011). Getting the measure of eutrophication in the Baltic Sea: towards improved assessment principles and methods. Biogeochemistry, 106(2), 137–156.

Attila, J., Kauppila, P., Kallio, K.Y., Alasalmi, H., Keto, V., Bruun, E and Koponen, S. Applicability of Earth Observation chlorophyll-a data in assessment of water status via MERIS — With implications for the use of OLCI sensors. Remote Sensing of Environment 212 (2018) 273–287. https://doi.org/10.1016/j.rse.2018.02.043

Bartlett, M. S. (1947) "The Use of Transformations." Biometrics, vol. 3, no. 1, pp. 39-52. JSTOR www.jstor.org/stable/3001536

Beasley TM, Erickson S, Allison DB (2009) Rank-based inverse normal transformations are increasingly used, but are they merited? Behav. Genet.; 39(5): 580-595. pmid:19526352

Berthon, J.-F., Zibordi, G. (2004) Bio-optical relationships for the northern Adriatic Sea. Int. J. Remote Sens., 25, 1527-1532.

COMMISSION DECISION (EU) 2018/229 of 12 February 2018 establishing, pursuant to Directive 2000/60/EC of the European Parliament and of the Council, the values of the Member State monitoring system classifications as a result of the intercalibration exercise and repealing Commission Decision 2013/480/EU.

HELCOM. (2010). Ecosystem health of the Baltic Sea 2003-2007: HELCOM Initial Holistic Assessment.

Pavlidou, A., N. Simboura, E. Rousselaki, M. Tsapakis, K. Pagou, P. Drakopoulou, G. Assimakopoulou, H. Kontoyiannis and P. Panayotidis (2015). "Methods of eutrophication assessment in the context of the water framework directive: Examples from the Eastern Mediterranean coastal areas." Continental Shelf Research 108: 156-168.

R Development Core Team (2023). R: A language and environment for statistical computing. R Foundation for Statistical Computing, Vienna, Austria. ISBN 3-900051-07-0. http://www.R-project.org

Simboura et al. (2015) Assessment of the environmental status in the Hellenic coastal waters (Eastern

Mediterranean): from the Water Framework Directive to the Marine Strategy Framework Directive. Medit. Mar. Sci., 16/1, 46-64

Van der Waerden BL. (1952) Order tests for the two-sample problem and their power. Ser A;55:453-458.

Volpe, G., Buongiorno Nardelli, B., Colella, S., Pisano, A. and Santoleri, R. (2018). An Operational Interpolated Ocean Colour Product in the Mediterranean Sea, in New Frontiers in Operational Oceanography, edited by E. P. Chassignet, A. Pascual, J. Tintorè, and J. Verron, pp. 227–244

Volpe, G., Colella, S., Brando, V. E., Forneris, V., Padula, F. L., Cicco, A. D., ... & Santoleri, R. (2019). Mediterranean ocean colour Level 3 operational multi-sensor processing. Ocean Science, 15(1), 127-146.